

## Scaling Relations Related to the Kinetics of Excimer Formation between Pyrene Groups Attached onto Poly(*N,N*-dimethylacrylamide)s

Sabesh Kanagalingam, John Spartalis, Tri-Minh Cao, and Jean Duhamel\*

*Institute for Polymer Research, Department of Chemistry, University of Waterloo,  
200 University Avenue West, Waterloo, Ontario N2L 3G1, Canada*

*Received May 22, 2002; Revised Manuscript Received July 26, 2002*

**ABSTRACT:** The fluorescence decays of the pyrene monomer of a series of pyrene-labeled poly(*N,N*-dimethylacrylamide)s (PyPDMAAm) were acquired in *N,N*-dimethylformamide (DMF) and acetone with different concentrations of nitromethane and at very low polymer concentration. DMF and acetone are good and mediocre solvents for PyPDMAAm, respectively. Nitromethane is a potent quencher of pyrene. Nitromethane addition to the polymer solution shortens the pyrene lifetime. The fluorescence decays of the quenched and unquenched pyrene-labeled polymers were analyzed with a blob model. Shortening the lifetime of pyrene reduces the volume probed by the dye while it remains excited. For each quencher concentration, the blob volume and size were determined, and scaling laws were shown to hold. The exponents retrieved from the scaling relationships agreed with those reported in polymer science textbooks.

### Introduction

An experimentalist aiming at characterizing polymer chain dynamics by fluorescence collisional quenching has no more than two options at hand. In the first option, a dye and its quencher are covalently attached at specific positions of the polymer chain. They can be located at the chain ends of a monodisperse polymer,<sup>1–4</sup> in which case end-to-end cyclization dynamics are monitored, or at internal positions separated by a well-defined polymer length,<sup>5,6</sup> which allows the investigation of intrachain dynamics. A wealth of information has been retrieved about polymer chain dynamics by using this approach. These experiments require that the polymeric chain spanning the dye and its quencher have a well-defined length, since the rate of encounter between a dye and its quencher depends strongly on the polymer chain length between the two species. A quantitative analysis of the fluorescence data is more complicated if the dye and quencher are attached at the ends of a polydisperse polymer. It is also interesting to note that only two units of the entire polymer chain are being probed in such an experiment, namely the two units bearing the dye and its quencher. In the case of a 10K polystyrene chain end-capped with a dye and its quencher, 98% of all monomer units constituting the chain are invisible.

In the second option, the dye and its quencher are randomly attached onto the polymer chain.<sup>7–11</sup> This procedure ensures that the entire chain is being probed. Unfortunately, the random labeling of the polymer chain leads to a distribution of chain lengths spanning dyes and quenchers, which yields an intractable number of encounter rate constants. Consequently, only qualitative information about polymer chain dynamics could be retrieved until recently.

Obviously, the ideal option consists of combining both aspects, i.e., randomly labeling the polymer chain to probe it in its entirety while still retrieving quantitative information from the analysis of the fluorescence data. This is now possible with the help of a blob model.<sup>11</sup> In

a blob-based analysis, the focus is the excited dye attached onto the polymer chain. While it remains excited, its motion is hindered by the chain already present inside the polymer coil and also by the mass of polymer it has to drag. Consequently, the excited dye does not move freely throughout the polymer coil during its lifetime but rather probes a well-defined volume, which is referred to as a blob. The polymer coil is then arbitrarily divided into identical blobs. Since the quenchers are randomly attached onto the polymer, they distribute themselves randomly among the blobs according to a Poisson distribution. The kinetics of encounter between an excited dye and the quenchers can be accounted for by using models that were initially developed for micellar systems,<sup>12,13</sup> the only difference being that the micelle is replaced by a polymeric blob. So far, the blob model has been successfully applied to describe the kinetics of encounter between pyrenes randomly attached onto polystyrene<sup>11a</sup> and poly(*N,N*-dimethylacrylamide).<sup>11b</sup> In these studies, the ground-state pyrene is the quencher of the excited pyrene. Diffusional encounter between the two leads to the formation of an excited complex called an excimer, which results in the disappearance of the excited monomer.<sup>14</sup>

Whether they are derived for linear,<sup>15</sup> star,<sup>16</sup> or branched<sup>17</sup> polymers or block copolymers in micelles,<sup>18</sup> blob models are always utilized to describe the scaling properties of polymer chains. Consequently, scaling laws must also be observed with the blob model developed for the fluorescence experiments described above. Since a blob represents the volume probed by an excited dye during its lifetime, altering the lifetime of the dye must affect the blob volume. As a result, a simple quenching experiment will yield a series of blob sizes, for which a scaling behavior should be observed. To this effect, a series of seven pyrene-labeled poly(*N,N*-dimethylacrylamide)s (PyPDMAAm) have been investigated in solutions containing increasing amounts of nitromethane, an efficient quencher for pyrene. Whether in dimethylformamide (DMF), a good solvent for PyPDMAAm or acetone, a mediocre solvent for PyPDMAAm,<sup>11b</sup> scaling

\* To whom correspondence should be addressed.

**Table 1. Weight-Average Molecular Weights (Determined by Static Light Scattering), Pyrene Content in mol %, and  $\lambda$  (mol of Pyrenes per g of Polymer) of Py-PDMAAm and PDMAAm (Determined by UV-vis Absorption)**

polymer	$\bar{M}_w$ (kg/mol)	pyrene content (mol %)	$\lambda$ ( $\mu\text{mol/g}$ )
PDMAAm	94	0.0	0
15Py-PDMAAm	80	0.2	15
100Py-PDMAAm	297	1.0	98
265Py-PDMAAm	165	2.7	263
350Py-PDMAAm	134	3.7	349
480Py-PDMAAm	123	5.2	479
570Py-PDMAAm	105	6.3	570
650Py-PDMAAm	105	7.3	645

laws are shown to hold between the parameters retrieved by the blob model.

Two types of quenchers are being used in this paper with very distinct purposes. The first quencher is nitromethane, which is a small molecule which dissolves homogeneously in the solvent. The quenching of the excited pyrene by nitromethane results in a shortening of the pyrene lifetime which is proportional to the nitromethane concentration. The second quencher is the ground-state pyrene. Since pyrene is randomly incorporated into the polymer backbone, pockets are generated inside the polymer coil which are either rich or poor in pyrene. This range of local pyrene concentrations inside the polymer coil leads to a distribution of rate constants for excimer formation which is handled by the blob model. In this study, the nitromethane quencher shortens the lifetime of the excited pyrene, which restricts the volume it can probe before being quenched by a ground-state pyrene. The introduction of nitromethane as a quencher to the polymer solution brings under scrutiny processes which occur over shorter time scales, a procedure which has already been used to probe the internal motions of macromolecules by fluorescence anisotropy.<sup>19</sup>

## Experimental Section

Most of the procedures used and syntheses carried out in this study have been already reported.<sup>11b</sup> They are succinctly reviewed hereafter.

**Chemicals.** The quality and source of all chemicals and solvents used in this study have been reported in an earlier publication.<sup>11b</sup>

**Synthesis of Poly(*N,N*-dimethylacrylamide-*co-N*-methylpyreneacrylamide) (PyPDMAAm).** The copolymers were synthesized by random copolymerization of *N*-methylpyreneacrylamide (PyMeAAm) and *N,N*-dimethylacrylamide in DMF. Details about the synthesis have been reported elsewhere.<sup>11b</sup> The copolymers were purified by dialysis followed by several precipitations. The weight-average molecular weights determined by static light scattering, and the pyrene contents determined by UV-vis absorption were obtained in an earlier publication<sup>11b</sup> and are listed in Table 1. The random incorporation of the comonomers into the growing polymer chain was confirmed earlier by <sup>1</sup>H NMR.<sup>11b</sup>

**Steady-State Fluorescence Measurements.** All fluorescence spectra were collected on a Photon Technology International LS-100 steady-state system with a pulsed xenon flash lamp as the light source. The spectra of all solutions were acquired with the usual right angle configuration. A gentle flow of nitrogen for 20 min was used to degas all solutions. The fluorescence intensities of the monomer ( $I_M$ ) and of the excimer ( $I_E$ ) were taken by measuring the integrals under the fluorescence spectra from 372 to 378 nm for the monomer and from 500 to 530 nm for the excimer. All samples were excited at 344 nm. The concentration in pyrene was kept at or below  $3 \times 10^{-6}$  M to avoid intermolecular excimer formation. The

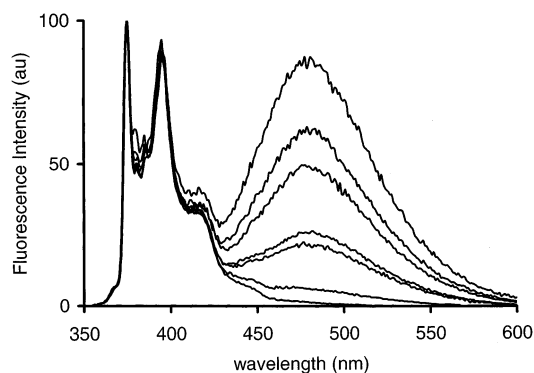


**Figure 1.** Fluorescence spectra of Py-PDMAAm with increasing pyrene contents in  $\lambda$  ( $\mu\text{mol/g}$ ) = 15, 100, 265, 350, 480, 570, and 645 (bottom to top). The spectra were normalized at 374 nm, which corresponds to the 0–0 peak. All samples were excited at 344 nm, and the pyrene concentration of these polymer solutions was  $\sim 3 \times 10^{-6}$  M.

same solution preparation was used for the time-resolved fluorescence experiments.

**Time-Resolved Fluorescence Measurements.** All fluorescence decay curves were recorded with a Photochemical Research Associates Inc. System 2000 by the time-correlated single photon counting technique. All samples were excited at 344 nm, and the fluorescence emission from the pyrene monomer and excimer were monitored at 375 and 510 nm, respectively. More information on this instrument is reported elsewhere.<sup>11</sup>

**Analysis of the Fluorescence Decays.** The fluorescence decays of the pyrene monomer were fitted by either a sum of exponentials (eq 1) or the blob model equation (eq 2). The parameters  $A_2$ ,  $A_3$ , and  $A_4$  are given in eq 3. The definition of the parameters  $k_{\text{blob}}$ ,  $^{20} \langle n \rangle$ , and  $k_e[\text{blob}]$  is given in the Results section. The parameter  $f$  in eq 2 represents the fraction of excited pyrene monomers which form excimer via diffusion.

$$i_M(t) = \sum_{i=1}^{n_{\text{exp}}} a_{M,i} \exp(-t/\tau_{M,i}) \quad n_{\text{exp}} = 2, 3 \quad (1)$$

$$i_M(t) = f \exp(-A_2 t - A_3 [1 - \exp(-A_4 t)]) + (1 - f) \exp(-t/\tau_{\text{AD}}) \quad (2)$$

where

$$A_2 = \langle n \rangle \frac{k_{\text{blob}} k_e [\text{blob}]}{k_{\text{blob}} + k_e [\text{blob}]} \quad A_3 = \langle n \rangle \frac{k_{\text{blob}}^2}{(k_{\text{blob}} + k_e [\text{blob}])^2} \quad A_4 = k_{\text{blob}} + k_e [\text{blob}] \quad (3)$$

Equation 2 was developed on the basis of the equations generally used to deal with micellar systems.<sup>12,13</sup> The random copolymerization introduces some PyMeAAm monomers next to one another on the polymer backbone. The close vicinity of these pyrene groups induces excimer formation on a subnanosecond time scale, which is too short to be probed by our time-resolved spectrofluorometer. This fast excimer formation process was accounted for in the analysis of the monomer fluorescence decays by using a light scattering correction.<sup>21</sup> The parameters of eqs 1 and 2 were optimized using the Marquardt–Levenberg algorithm.<sup>22</sup>

## Results

Figure 1 represents the fluorescence spectra of PyPDMAAm in DMF with increasing pyrene contents. The fluorescence experiments were performed with a pyrene concentration of  $3 \times 10^{-6}$  M to ensure that excimer is formed intramolecularly. As more pyrene is attached onto the polymer backbone, more intramolecu-

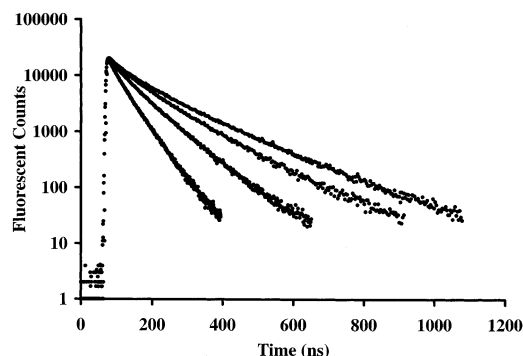


**Figure 2.** Monomer fluorescence decays of pyrene ( $\lambda_{\text{ex}} = 344$  nm,  $\lambda_{\text{em}} = 375$  nm) for 350-PyPDMAAm with nitromethane concentrations 0, 0.00092, 0.0035, and 0.0078 M in DMF. Nitromethane content increases from right to left. The pyrene concentration of these polymer solutions in DMF was  $\sim 3 \times 10^{-6}$  M.

**Table 2. Summary of the Parameters Retrieved by the Blob Model Analysis of the Monomer Fluorescence Decays with and without Nitromethane Quencher**

solvent, [quencher]/mM	$\eta$ ( $10^3$ Pa·s)	$\tau$ (ns)	$k_{\text{blob}}$ ( $10^7$ s $^{-1}$ )	$N_{\text{blob}}$
acetone	0.31	256	$0.9 \pm 0.1$	$60 \pm 6$
acetone, 0.9	0.31	170	$1.1 \pm 0.1$	$49 \pm 3$
acetone, 3.1	0.31	100	$1.5 \pm 0.2$	$41 \pm 2$
acetone, 8.2	0.31	46	$2.4 \pm 0.2$	$29 \pm 1$
DMF	0.79	220	$1.1 \pm 0.1$	$26 \pm 2$
DMF, 1.0	0.79	165	$1.3 \pm 0.2$	$26 \pm 1$
DMF, 3.5	0.79	99	$1.7 \pm 0.1$	$21 \pm 3$
DMF, 7.8	0.79	57	$2.1 \pm 0.2$	$19 \pm 2$

lar encounters take place between an excited pyrene and a ground-state pyrene and more excimer forms.

The effect of quencher concentration on the fluorescence decay of the pyrene monomer is shown in Figure 2. With increasing quencher concentration, the lifetime of the pyrene monomer decreases. Nitromethane has been used by others as a nonionic quencher suited for organic solvents.<sup>23</sup> The natural lifetime of the pyrene monomer ( $\tau_M^\circ$ ) attached onto the pyrene backbone was determined from the biexponential fits of 15-PyPDMAAm decays in acetone and DMF with eq 1. The copolymer 15-PyPDMAAm has a very low pyrene content, and most of the pyrenes exist as isolated monomers. Thus, very little excimer is being formed with this polymer sample. The fluorescence decays of 15-PyPDMAAm in acetone and DMF fitted with a sum of two exponentials yield a long decay time with a contribution which accounts for at least 85% of the total preexponential weight. This long decay time  $\tau_M^\circ$  was found to equal 256 and 220 ns in acetone and DMF, respectively. Upon quenching by nitromethane,  $\tau_M^\circ$  reduces to  $\tau_M$ . A Stern–Volmer plot of  $\tau_M^\circ/\tau_M$  vs nitromethane concentration yields a straight line. The bimolecular quenching rate constant ( $k_Q$ ) by nitromethane is found to equal  $2.2 \times 10^9$  and  $1.7 \times 10^9$  M $^{-1}$  s $^{-1}$  in acetone and DMF, respectively.

Quenching of pyrene by nitromethane provides a means to control the pyrene lifetime. The largest decrease in lifetime between the polymer with no quencher and the highest quencher concentration ( $\tau_M^\circ/\tau_M$ ) was 5.6 in acetone whereas in DMF the largest ratio  $\tau_M^\circ/\tau_M$  was slightly lower at 3.9 (cf. Table 2). According to the framework of the blob model, an excited pyrene with a shorter lifetime probes a smaller volume in the polymer coil. Consequently, quenching of pyrene by nitromethane is expected to affect the blob size ( $N_{\text{blob}}$ )

and the blob volume ( $V_{\text{blob}}$ ) retrieved from the analysis of the fluorescence decays. These trends are investigated in the Discussion section.

All monomer fluorescence decays with different nitromethane concentrations in acetone and DMF were fitted with eq 2. The fits were good with  $\chi^2$  smaller than 1.30. The blob model describes the kinetics of excimer formation inside the polymer coil with three parameters, namely, the average number of pyrene groups in a blob,  $\langle n \rangle$ , the rate constant of excimer formation inside a blob,  $k_{\text{blob}}$ ,<sup>20</sup> and the rate at which pyrene groups exchange from blob to blob,  $k_e[\text{blob}]$ , where  $k_e$  is the exchange rate constant and  $[\text{blob}]$  is the blob concentration inside the polymer coil.<sup>11</sup> The results obtained from the fits for all polymer systems are listed in Table 3. In Table 3, the parameter  $f$  represents the fraction of pyrenes that are located in a pyrene-rich region of the polymer coil and form excimer during the lifetime of the excited pyrene (cf. eq 2).<sup>11</sup>

## Discussion

The PyPDMAAm series was studied in acetone and DMF for two reasons. First, both solvents are good solvents for the pyrene moieties so that little ground-state pyrene associations are present and excimer is formed essentially by diffusion.<sup>11b</sup> As a first approximation, each pyrene moiety can be considered as a potential quencher of the excited pyrene, and the pyrene  $\rightleftharpoons$  quencher equivalence is believed to hold in acetone and DMF.<sup>11b</sup> The existence of pyrene ground-state associations usually complicates a blob model analysis of the fluorescence decays since an aggregate of ground-state pyrenes can act as a single quenching entity. In that case, there would be less quenchers in the polymer coil than there are pyrenes. Second, the solvent quality of acetone and DMF toward PyPDMAAm has been shown to be mediocre and good, respectively.<sup>11b</sup> Consequently, the polymer coil is expected to adopt a conformation that is more collapsed in acetone than in DMF. Since different scaling behaviors are expected for polymers dissolved in solvents having different quality, one would expect those different scaling behaviors to be probed by a blob model analysis. The parameters  $k_{\text{blob}}$  and  $N_{\text{blob}}$ , which are discussed in the following section, were found to remain constant for a given quencher concentration regardless of pyrene content, and only their average values are reported in the text and figures. The reported error bars represent the standard deviations calculated from the results retrieved for the entire PyPDMAAm series at a given nitromethane concentration.

**Encounter Rate Constant ( $k_{\text{blob}}$ ).** The rate constant  $k_{\text{blob}}$  characterizes the diffusion-controlled formation of excimer between one excited pyrene and one ground-state pyrene, both located inside the same blob.<sup>11,20</sup> A plot of  $k_{\text{blob}}^{-1}$  as a function of the pyrene lifetime in acetone and DMF is shown in Figure 3. Within experimental error,  $k_{\text{blob}}^{-1}$  increases linearly with the pyrene lifetime. Interestingly, despite the fact that DMF ( $\eta_{25^\circ\text{C}} = 0.79$  mPa·s) is 2.5 times more viscous than acetone ( $\eta_{25^\circ\text{C}} = 0.31$  mPa·s), a single curve is obtained in both solvents. The parameter  $k_{\text{blob}}^{-1}$  is not viscosity-controlled! At first sight, this result is surprising because diffusion-controlled excimer formation usually imposes that the rate of excimer formation be inversely proportional to the viscosity.

The explanation for this unexpected result is found in the very definition of  $k_{\text{blob}}$ . The rate constant for



**Table 3. Parameters Retrieved from the Blob Model Analysis of the Pyrene Monomer Fluorescence Decays of Py-PDMAAm in Acetone and DMF According to Eq 2**

solvent	polymer	<i>f</i>	<i>k</i> <sub>blob</sub> (10 <sup>7</sup> s <sup>-1</sup> )	⟨ <i>n</i> ⟩	<i>k</i> <sub>e</sub> [blob] (10 <sup>7</sup> s <sup>-1</sup> )	χ <sup>2</sup>
acetone	100Py-PDMAAm	0.74	0.93	0.84	0.44	1.15
	265Py-PDMAAm	0.97	0.74	1.98	0.42	1.09
	350Py-PDMAAm	0.96	0.79	2.30	0.46	1.18
	480Py-PDMAAm	0.99	0.95	2.92	0.68	1.14
	570Py-PDMAAm	0.99	0.89	3.75	0.45	1.01
	650Py-PDMAAm	0.99	1.13	3.74	0.68	1.15
acetone 0.9 mM	100Py-PDMAAm	0.66	1.10	0.80	0.51	1.04
	265Py-PDMAAm	0.94	1.08	1.55	0.73	1.13
nitromethane	350Py-PDMAAm	0.93	0.97	1.84	0.58	1.15
	480Py-PDMAAm	0.99	1.14	2.56	0.75	0.92
	570Py-PDMAAm	0.98	1.24	2.89	0.77	1.00
	650Py-PDMAAm	0.99	1.32	3.42	0.74	1.12
acetone 3.1 mM	100Py-PDMAAm	0.58	1.91	0.62	1.49	1.11
	265Py-PDMAAm	0.92	1.57	1.21	1.32	1.16
nitromethane	350Py-PDMAAm	0.94	1.24	1.62	0.98	1.21
	480Py-PDMAAm	0.98	1.42	2.18	1.19	1.08
	570Py-PDMAAm	0.99	1.44	2.62	1.00	1.21
	650Py-PDMAAm	0.99	1.62	3.01	1.02	1.12
acetone 8.4 mM	100Py-PDMAAm <sup>a</sup>	0.43				
	265Py-PDMAAm	0.85	2.51	0.95	1.93	1.14
nitromethane	350Py-PDMAAm	0.87	2.01	1.18	1.98	1.10
	480Py-PDMAAm	0.96	2.20	1.55	1.87	1.11
	570Py-PDMAAm	0.99	2.63	1.73	1.73	1.28
	650Py-PDMAAm	0.99	2.63	2.20	1.47	1.21
DMF	100Py-PDMAAm <sup>a</sup>	0.40				
	265Py-PDMAAm	0.86	1.14	0.86	0.64	0.98
	350Py-PDMAAm	0.88	1.10	1.02	0.58	0.91
	480Py-PDMAAm	0.96	1.22	1.30	0.68	0.88
	570Py-PDMAAm	0.97	1.04	1.70	0.64	1.16
	650Py-PDMAAm	0.99	1.20	2.10	0.77	1.03
DMF 1.0 mM	100Py-PDMAAm <sup>a</sup>	0.52				
	265Py-PDMAAm	0.85	1.46	0.82	0.81	1.27
nitromethane	350Py-PDMAAm	0.89	1.12	1.05	0.61	1.23
	480Py-PDMAAm	0.96	1.15	1.41	0.76	1.20
	570Py-PDMAAm	0.97	1.26	1.61	0.83	1.01
	650Py-PDMAAm	0.99	1.50	1.94	0.89	1.21
DMF 3.5 mM	100Py-PDMAAm <sup>a</sup>	0.51				
	265Py-PDMAAm	0.80	1.52	0.83	1.16	1.08
nitromethane	350Py-PDMAAm	0.82	1.79	0.88	1.02	1.08
	480Py-PDMAAm	0.82	1.58	1.14	0.94	1.11
	570Py-PDMAAm	0.96	1.72	1.31	1.22	0.93
	650Py-PDMAAm	0.97	1.79	1.68	1.47	1.24
DMF 7.8 mM	100Py-PDMAAm <sup>a</sup>	0.38				
	265Py-PDMAAm	0.77	1.82	0.79	1.17	1.09
nitromethane	350Py-PDMAAm	0.85	2.24	0.76	1.28	0.99
	480Py-PDMAAm	0.98	1.94	1.01	1.19	0.87
	570Py-PDMAAm	0.93	2.17	1.15	1.81	0.94
	650Py-PDMAAm	0.94	2.43	1.36	1.65	1.02

<sup>a</sup> The contribution from unquenched pyrenes is too large to retrieve meaningful parameters from the blob model analysis.

excimer formation (*k*<sub>blob</sub>) between one excited pyrene and one ground-state pyrene both located inside a blob is a pseudo-unimolecular rate constant. As in micelles where the rate constant for excimer formation is also a pseudo-unimolecular rate constant,<sup>12,13</sup> *k*<sub>blob</sub> is really the product of a rate constant for excimer formation *k* time the concentration of one ground-state pyrene inside a blob; in other words, *k*<sub>blob</sub> = *k*(1pyrene/*V*<sub>blob</sub>) = *k*/*V*<sub>blob</sub>. To rationalize the behavior of *k*<sub>blob</sub>, both parameters *k* and *V*<sub>blob</sub> must be considered. Assuming that the pyrene pendants forming excimer are separated far enough on the backbone to ensure diffusional encounters, *k* will be inversely proportional to the solvent viscosity (*k* ∼ *η*<sup>-1</sup>). The blob volume combines a dynamic component with a physical component. Because of its definition, *V*<sub>blob</sub> depends on how far a chromophore attached onto the polymer backbone will diffuse in solution. Consequently, the blob volume is inversely proportional to the solvent viscosity. This is the dynamic aspect of *V*<sub>blob</sub>. But the blob volume has also a physical volume, which should depend on the number of monomers making up

a blob, i.e., *N*<sub>blob</sub>. This represents the physical aspect of *V*<sub>blob</sub>. As a first approximation, one can assume that the physical volume of a blob scales as *N*<sub>blob</sub><sup>3ν</sup>, a well-known relationship derived for polymer coils and assumed to be valid for any theory involving a blob model, where ν equals 0.5 in a poor solvent and 0.6 in a good solvent.<sup>15–18</sup> Taking into account the physical and dynamic components of *V*<sub>blob</sub>, the blob volume is expected to scale as *N*<sub>blob</sub><sup>3ν/η</sup>. Consequently, the following relationship is expected for the pseudo-unimolecular rate constant *k*<sub>blob</sub>.

$$k_{\text{blob}} = \frac{k}{V_{\text{blob}}} \sim \frac{\eta^{-1}}{\eta^{-1} N_{\text{blob}}^{3\nu}} = N_{\text{blob}}^{-3\nu} \quad (4)$$

This relationship implies that *k*<sub>blob</sub> does not depend on solvent viscosity and is inversely proportional to the physical volume of a blob. The trend shown in Figure 3 agrees with this statement. A 2.5 increase in viscosity when switching the solvent from acetone to DMF does not affect *k*<sub>blob</sub>, but *k*<sub>blob</sub><sup>-1</sup> which is proportional to the

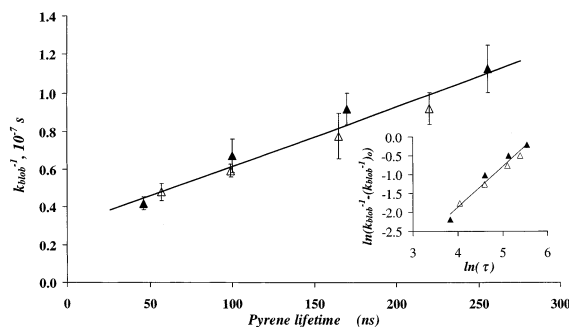


**Figure 3.** Plot of  $k_{\text{blob}}^{-1}$  (averaged for the entire PyPDMAAm series studied for a particular quencher concentration with standard deviation indicated by the error bars) vs the pyrene lifetime in both acetone and DMF. The pyrene concentration of these polymer solutions in DMF was  $\sim 3 \times 10^{-6}$  M ( $\blacktriangle$  in acetone and  $\triangle$  in DMF). Inset: plot of  $\ln(k_{\text{blob}}^{-1} - (k_{\text{blob}}^{-1})_0)$  vs  $\ln(\tau)$  obtained in both acetone ( $\blacktriangle$ ) and DMF ( $\triangle$ ). The standard deviations on the mean are indicated by the error bars.

physical size of a blob increases for a longer-lived pyrene since it can probe a bigger volume inside the polymer coil.

Another interesting point in Figure 3 is that  $k_{\text{blob}}^{-1}$  does not equal zero when the pyrene lifetime equals zero, which implies in other words that an excited pyrene can probe a finite volume even if its lifetime equals zero. This inconsistency is a result of a switch occurring in the way the excimer is being formed. When the pyrene lifetime shortens, only those pyrenes that are very close to one another can form excimer. Zachariasse and co-workers have clearly established that the process of excimer formation between two pyrene groups located at the ends of short oligomethylene chains is not diffusion-controlled.<sup>24</sup> Thus, it is expected that excimer formation occurs via local polymer motions of the polymer backbone when an excited pyrene probes short distances; i.e., its lifetime is short. As the pyrene lifetime lengthens, excimer formation becomes diffusion-controlled. This is the diffusion-controlled process of excimer formation, which is being probed in Figure 3.

A similar conclusion was drawn from the study of the excimer formation process of poly(methyl methacrylate) randomly labeled with pyrene as a function of viscosity.<sup>8a</sup> Excimer formation was found to be diffusion-controlled at low viscosity and non-diffusion-controlled at high viscosity. This is because at high viscosity, only those pyrenes close to one another can form excimer, and this process occurs via local polymer motions.

**Probing Volume ( $V_{\text{blob}}$ ) and Size ( $N_{\text{blob}}$ ).** According to eq 4,  $k_{\text{blob}}^{-1}$  is proportional to  $V_{\text{blob}} \sim N_{\text{blob}}^{3\nu}$ . As the pyrene lifetime increases,  $V_{\text{blob}}$  increases and so does  $k_{\text{blob}}^{-1}$  as shown in Figure 3. The size of a blob, i.e., the number of monomer units making up a blob, can be determined from the blob model analysis. This is achieved by using eq 5, where  $\lambda$  is the pyrene content of the pyrene-labeled polymer (in moles of pyrenes per gram of polymer) determined by UV-vis measurements, and  $f$  and  $\langle n \rangle$  are retrieved from the analysis of the fluorescence decays with eq 2. Their values have been listed in Table 3.

$$N_{\text{blob}} = \frac{\langle n \rangle}{\lambda / f (285x + 99(1 - x))} \quad (5)$$

The term  $(285x + 99(1 - x))$  in the denominator of eq 5 accounts for the number-average molar mass of the

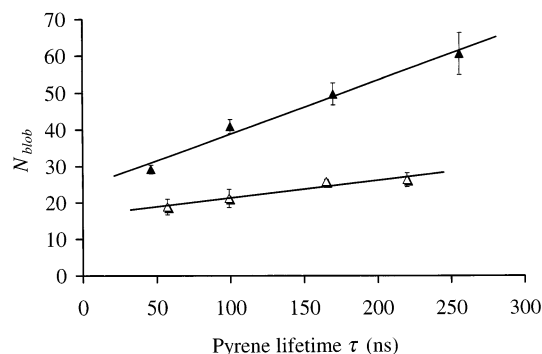


**Figure 4.** Plot of  $N_{\text{blob}}$  (averaged for the entire PyPDMAAm series studied for a particular quencher concentration with standard deviation indicated by the error bars) vs the pyrene lifetime in both acetone and DMF. The pyrene concentration of these polymer solutions in DMF was  $\sim 3 \times 10^{-6}$  M ( $\blacktriangle$  in acetone and  $\triangle$  in DMF).

monomer unit where  $x$  is the content of PyMeAAm in mol %. The correction  $1/f$ , where  $f$  is the fraction of pyrenes that do form excimer by diffusion (cf. eq 2), accounts for the fact that some domains of the polymer coil are poor in pyrene and do not contribute to the process of excimer formation.<sup>11</sup> Except for 100-PyPDMAAm,  $f$  is usually close to 1.0, and the ratio  $\lambda/f$  takes a value that is close to the nominal pyrene content of the polymer ( $\lambda$ ).

For each quencher concentration, the  $N_{\text{blob}}$  value remains constant within experimental error. It is plotted as a function of the pyrene lifetime in Figure 4. As nitromethane is added to the solution, the pyrene lifetime is shortened; the excited pyrene probes a smaller volume as shown in Figure 3 (where  $k_{\text{blob}}^{-1} \propto V_{\text{blob}}$  decreases with shorter lifetime), and  $N_{\text{blob}}$  decreases. There is thus qualitative agreement between Figures 3 and 4. However, whereas  $k_{\text{blob}}^{-1}$  is the same in acetone and DMF,  $N_{\text{blob}}$  is significantly smaller in DMF than in acetone. If  $k_{\text{blob}}^{-1}$  is indeed proportional to  $V_{\text{blob}}$ , the trends shown in Figures 3 and 4 indicate that the polymer coil is denser in acetone than in DMF. This conclusion is in agreement with the respective quality of acetone (mediocre) and DMF (good) toward PyPDMAAm.<sup>11b</sup>

Although  $N_{\text{blob}}$  increases linearly with the pyrene lifetime, a straight line drawn through  $N_{\text{blob}}$  does not go through the origin. In fact, a linear relationship between the pyrene lifetime and  $N_{\text{blob}}$  would require that, at zero probing time ( $\tau_M = 0$  ns),  $N_{\text{blob}}$  be 24 and 16 monomer units in acetone and DMF, respectively. This observation is similar to that observed with  $k_{\text{blob}}^{-1}$  in Figure 3. This result is rationalized in the same manner. For very short lifetimes, the probing region is limited to a few monomer units, and the kinetics of encounter between two pyrene groups becomes strongly dependent on chain conformation. In effect, local polymer motions control the excimer formation process for short pyrene lifetimes. As the lifetime lengthens, the encounters become diffusion-controlled, and this is the regime monitored in Figures 3 and 4.

**Scaling Laws.** Any derivation using blobs to describe scaling relationships with polymeric systems requires that  $V_{\text{blob}} \sim N_{\text{blob}}^{3\nu}$ , where  $\nu$  equals 0.5 and 0.6 in a  $\Theta$  and good solvent, respectively. This relationship implies that a plot of  $V_{\text{blob}}$  as a function of  $N_{\text{blob}}$  passes through the origin. Although plots of  $V_{\text{blob}}$  ( $\propto k_{\text{blob}}^{-1}$ ) and  $N_{\text{blob}}$  do not go through the origin when graphed against the

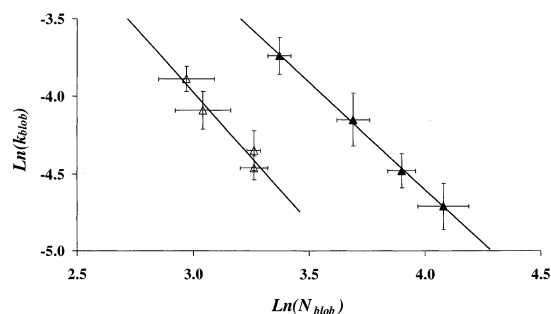


**Figure 5.** Plot of  $\ln(k_{\text{blob}})$  vs  $\ln(N_{\text{blob}})$  obtained in both acetone ( $\blacktriangle$ ) and DMF ( $\triangle$ ). The standard deviations on the mean are indicated by the error bars. The slopes equal  $-1.8 \pm 0.3$  in DMF and  $-1.4 \pm 0.2$  in acetone.

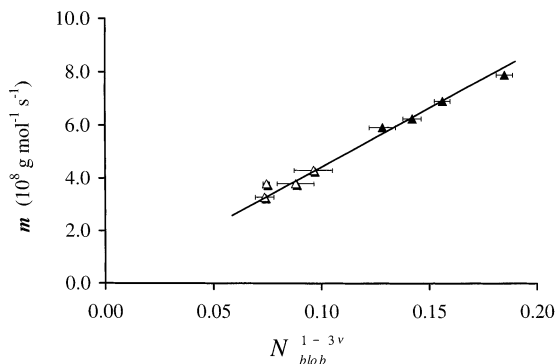


**Figure 6.** Slope  $m$  of plots of  $k_{\text{blob}}\langle n \rangle$  vs  $(\lambda/f)$  is plotted as a function of  $N_{\text{blob}}^{1-3\nu}$ .

lifetime  $\tau_M$  (cf. Figures 3 and 4), a power law plot of  $V_{\text{blob}}$  vs  $N_{\text{blob}}$  does pass through the origin (plot shown in Supporting Information). This is because all the data reported in this study such as  $V_{\text{blob}}$  and  $N_{\text{blob}}$  deal with the diffusion-controlled regime of excimer formation. Consequently, scaling relationships can be derived between these two parameters.

Since  $k_{\text{blob}}^{-1}$  describes the volume probed by an excited pyrene during its lifetime and  $N_{\text{blob}}$  yields the number of units inside a blob, one is tempted to investigate whether  $k_{\text{blob}}$  scales as  $N_{\text{blob}}^{-3\nu}$ , as suggested by eq 4. A plot of  $\ln(k_{\text{blob}})$  as a function of  $\ln(N_{\text{blob}})$  yields two straight lines in acetone and DMF as shown in Figure 5. The slopes of the straight lines equal  $-1.4 \pm 0.2$  and  $-1.8 \pm 0.3$  in acetone and DMF, respectively. These values are remarkably close to what would be expected for a  $\Theta$  solvent (acetone) and a good solvent (DMF) where  $3\nu$  would equal 1.5 and 1.8, respectively.

A second scaling relationship can be derived with the product  $k_{\text{blob}}\langle n \rangle$ . Since  $k_{\text{blob}}$  is inversely proportional to  $V_{\text{blob}}$  and  $\langle n \rangle$  is the average number of pyrenes per blob, the product  $k_{\text{blob}}\langle n \rangle$  represents the local pyrene concentration inside the polymer coil. According to eq 4,  $k_{\text{blob}}$  scales as  $N_{\text{blob}}^{-3\nu}$  whereas  $\langle n \rangle$  scales as  $(\lambda/f)N_{\text{blob}}$  according to eq 5. Consequently, the product  $k_{\text{blob}}\langle n \rangle$  is expected to scale as  $(\lambda/f)N_{\text{blob}}^{1-3\nu}$ , where  $\nu$  is taken to equal 0.5 and 0.6 in acetone and DMF, respectively. For each quencher concentration, plots of  $k_{\text{blob}}\langle n \rangle$  vs the corrected pyrene content  $(\lambda/f)$  yield straight lines with slopes  $m$ . When the slope  $m$  is plotted as a function of  $N_{\text{blob}}^{1-3\nu}$  in Figure 6, a linear relationship is obtained, confirming that the product  $k_{\text{blob}}\langle n \rangle$  scales as  $(\lambda/f)N_{\text{blob}}^{1-3\nu}$ .

In 1967, de Gennes showed that the random distance  $\Delta x$  travelled by a unit of a polymer chain in solution during a time  $t$  is proportional to  $t^{1/4}$ .<sup>25</sup>  $k_{\text{blob}}^{-1}$  is proportional to the volume probed by an excited dye

during its lifetime. Consequently,  $k_{\text{blob}}^{-1}$  is proportional to  $\Delta x^3$  and should scale as  $\tau_M^{3/4}$  according to de Gennes' derivation. Experimentally,  $k_{\text{blob}}^{-1}$  was found to increase linearly with  $\tau_M$  as shown in Figure 3, but because of a change in regime,  $k_{\text{blob}}^{-1}$  intercepts the  $y$ -axis at  $(k_{\text{blob}}^{-1})_0 = 0.3 \times 10^{-7} \text{ s}^{-1}$ . To account for the nonzero intercept of Figure 3, a plot of  $\ln(k_{\text{blob}}^{-1} - (k_{\text{blob}}^{-1})_0)$  vs  $\ln(\tau_M)$  is shown in the inset of Figure 3. The slope of the straight line equals  $1.0 \pm 0.2$ . The scaling exponent agrees qualitatively with the de Gennes' prediction of 0.75.

**Implications.** Combining the quenching experiments with the blob model analysis provides a quantitative measurement of how far one unit of a polymer chain will travel during a finite time. According to Figure 4, one expects the following relationships to exist between the time a given dye remains excited and the number of units making up the volume of a PyPDMAAm polymer coil probed by this dye.

$$\text{in acetone: } \tau_M (\text{ns}) = 7.1(N_{\text{blob}} - 24) \quad (6a)$$

$$\text{in DMF: } \tau_M (\text{ns}) = 20.8(N_{\text{blob}} - 16) \quad (6b)$$

The numbers 24 and 16 in eqs 6 are due in part to the local polymer motions which occur very rapidly, allowing a monomer unit to probe a region of the polymer coil made of 24 units in acetone and 16 units in DMF. These numbers might also account for the bulkiness of the pyrene dyes whose size is equivalent to several monomer units. Nevertheless, one can conclude from these trends that any motion taking a monomer unit farther away from these restricted regions (24 monomer units in acetone and 16 monomer units in DMF) is diffusion-controlled and occurs on a much slower time scale. In the diffusion regime, eqs 6 predict that, in order to probe a volume made of 100 monomer units, the dye must remain excited for 540 and 1750 ns in acetone and DMF, respectively. In other terms, it will take 1750 ns for one unit of the PyPDMAAm backbone to have a chance of encountering any other monomer units of a 100 unit ensemble of the PyPDMAAm polymer coil in DMF. Such considerations can be used toward the prediction of whether two specific units along a polymer backbone can encounter during a finite time, with potential applications to protein folding and, as we already demonstrated, to associative polymers.<sup>26</sup> Furthermore, the data shown in Figure 5 also allow us to predict the trajectory of a given monomer undergoing diffusion inside a polymer coil.

The blob model was developed to monitor the kinetics of encounter between pendants randomly distributed along a polymer backbone. Its basic framework has been shown to apply to a series of pyrene-labeled polystyrenes<sup>11a</sup> and more recently to a series of pyrene-labeled poly(*N,N*-dimethylacrylamide)s.<sup>11b</sup> It has been used to determine the level of association of various water-soluble<sup>26a</sup> and oil-soluble associative polymers.<sup>26b</sup> Since blob models are introduced to account for the scaling behaviors of polymeric systems, evidence that the blob model used in this study could do so had been sorely missing in the literature. Figures 5 and 6 demonstrate that the parameters retrieved by the blob model obey scaling laws with scaling exponents which agree with those expected in polymer science. These conclusions identify the blob model as being a robust tool to study polymer chain dynamics by fluorescence spectroscopy.



## Conclusions

The fluorescence decays of the pyrene monomer of several PyPDMAAs were acquired in acetone and DMF with various amounts of nitromethane, an efficient quencher of the excited pyrene. The fluorescence decays were analyzed with the blob model. The rate constant for encounter between one excited pyrene and one ground-state pyrene inside a blob ( $k_{\text{blob}}$ ) was not affected by solvent viscosity but was found to increase with shorter lifetimes. The insensitivity of  $k_{\text{blob}}$  toward solvent viscosity is due to two effects which cancel each other out. A viscous solvent slows the dynamics of encounters as well as reduces the distance over which encounters can occur. Close encounters should occur at a faster rate, but they are slowed by the high viscosity. The increase of  $k_{\text{blob}}$  with shorter lifetime is explained by the blob model prediction that  $k_{\text{blob}}$  is inversely proportional to the blob volume. As the lifetime shortens, the excited dye probes a smaller volume and the encounters occur at a higher rate.

The blob size ( $N_{\text{blob}}$ ), which represents the number of monomer units inside a blob, was shown to increase with the lifetime in the same manner as  $k_{\text{blob}}^{-1}$ . The parameter  $k_{\text{blob}}$  scales as  $N_{\text{blob}}^{-3\nu}$ , where  $\nu$  equals 0.5 in a mediocre solvent (acetone) and 0.6 in a good solvent (DMF). Plots of  $k_{\text{blob}}\langle n \rangle$  vs the corrected pyrene content ( $\lambda/f$ ), ( $\langle n \rangle$  being the average number of pyrene per blob, yielded straight lines whose slopes  $m$  scale as  $N_{\text{blob}}^{1-3\nu}$ . These experiments establish that despite its empirical nature, the blob model yields trends that obey the well-accepted scaling laws observed in polymer science.

**Acknowledgment.** The authors thank NSERC for generous funding. J.D. is especially thankful to the financial help provided by his being awarded a Tier-2 Canada Research Chair.

**Supporting Information Available:** A power law plot of  $k_{\text{blob}}$  as a function of  $N_{\text{blob}}$ . This material is available free of charge via the Internet at <http://pubs.acs.org>.

## References and Notes

- Cuniberti, C.; Perico, A. *Eur. Polym. J.* **1977**, *13*, 369–374.
- Winnik, M. A.; Redpath, T.; Richards, D. H. *Macromolecules* **1980**, *13*, 328–335. Redpath, A. E. C.; Winnik, M. A. *J. Am. Chem. Soc.* **1980**, *102*, 6869–6871. Redpath, A. E. C.; Winnik, M. A. *J. Am. Chem. Soc.* **1982**, *104*, 5604–5607. Winnik, M. A.; Sinclair, A. M.; Beinert, G. *Can. J. Chem.* **1985**, *63*, 1300–1307. Winnik, M. A.; Redpath, A. E. C.; Paton, K.; Danhelka, J. *Polymer* **1984**, *25*, 91–99. Martinho, J. M. G.; Winnik, M. A. *Macromolecules* **1986**, *19*, 2281–2284. Martinho, J. M. G.; Reis e Sousa, A. T.; Winnik, M. A. *Macromolecules* **1993**, *26*, 4484–4488.
- Reis e Sousa, A. T.; Castanheira, E. M. S.; Fedorov, A.; Martinho, J. M. G. *J. Phys. Chem. A* **1998**, *102*, 6406–6411.
- Kane, M. A.; Baker, G. A.; Pandey, S.; Maziarz III, E. P.; Hoth, D. C.; Bright, F. V. *J. Phys. Chem. B* **2000**, *104*, 8585–8591.
- Lee, S.; Winnik, M. A.; Whittall, R. M.; Li, L. *Macromolecules* **1996**, *29*, 3060–3072. Lee, S.; Winnik, M. A. *Macromolecules* **1997**, *30*, 2633–2641.
- Brauge, L.; Caminade, A.-M.; Majoral, J.-P.; Slomkowski, S.; Wolszczak, M. *Macromolecules* **2001**, *34*, 5599–5606.
- Cuniberti, C.; Perico, A. *Eur. Polym. J.* **1980**, *16*, 887–893.
- (a) Wang, F. W.; Lowry, R. E. *Polymer* **1985**, *26*, 1046–1052. (b) Wang, F. W.; Lowry, R. E.; Cavanagh, R. R. *Polymer* **1985**, *26*, 1657–1661.
- Turro, N. J.; Arora, K. S. *Polymer* **1986**, *27*, 783–796.
- Anghel, D. F.; Alderson, V.; Winnik, F. M.; Mizusaki, M.; Morishima, Y. *Polymer* **1998**, *39*, 3035–3044.
- (a) Mathew, A. K.; Siu, H.; Duhamel, J. *Macromolecules* **1999**, *32*, 7100–7108. (b) Kanagalingam, S.; Ngan, C. F.; Duhamel, J. *Macromolecules*, in press.
- Tachiya, M. *Chem. Phys. Lett.* **1975**, *33*, 289–292.
- Infelta, P. P.; Gratzel, M.; Thomas, J. K. *J. Phys. Chem.* **1974**, *78*, 190–195.
- Birks, J. B. *Photophysics of Aromatic Molecules*; Wiley: New York, 1970; pp 301–371.
- Daoud, M.; Cotton, J. P.; Farnoux, B.; Jannink, G.; Sarma, G.; Benoit, H.; Duplessix, R.; Picot, C.; de Gennes, P. G. *Macromolecules* **1975**, *8*, 804–818. de Gennes, P. G. In *Scaling Concepts in Polymer Physics*; Cornell University Press: Ithaca, NY, 1979.
- Daoud, M.; Cotton, J. P. *J. Phys. (Paris)* **1982**, *43*, 531–538.
- Daoud, M.; Joanny, J. F. *J. Phys. (Paris)* **1981**, *42*, 1359–1371.
- Halperin, A. *Macromolecules* **1987**, *20*, 2943–2946.
- Bentz, J. P.; Beyl, J. P.; Beinert, G.; Weill, G. *Eur. Polym. J.* **1975**, *11*, 711–718.
- In previous publications from this laboratory, the rate of excimer formation inside a blob was referred to as  $k_{\text{diff}}$ . It was pointed out by an unknown referee that since the process of excimer formation inside a blob does not depend on viscosity, the choice of  $k_{\text{diff}}$  as a mathematical symbol was not appropriate and confusing to the reader. Consequently, we have been using the symbol  $k_{\text{blob}}$  instead of  $k_{\text{diff}}$ .
- Demas, J. N. *Excited-State Lifetime Measurements*; Academic Press: New York, 1983; p 134.
- Press, W. H.; Flannery, B. P.; Teukolsky, S. A.; Vetterling, W. T. *Numerical Recipes. The Art of Scientific Computing (Fortran Version)*; Cambridge University Press: Cambridge, 1992; pp 523–528.
- Olea, A. F.; Thomas, J. K. *J. Am. Chem. Soc.* **1988**, *110*, 4494–4502.
- Reynders, P.; Kühnle, W.; Zachariasse, K. A. *J. Am. Chem. Soc.* **1990**, *112*, 3929–3939. Zachariasse, K. A.; Maçanita, A. L.; Kühnle, W. *J. Phys. Chem. B* **1999**, *103*, 9356–9365.
- de Gennes, P.-G. *Physics* **1967**, *1*, 37–45. de Gennes, P.-G. *J. Chem. Phys.* **1982**, *76*, 3316–3321.
- (a) Prazeres, T. J. V.; Beingessner, R.; Duhamel, J.; Olesen, K.; Shay, G.; Bassett, D. R. *Macromolecules* **2001**, *34*, 7876–7884. (b) Vangani, V.; Drage, J.; Mehta, J.; Mathew, A. K.; Duhamel, J. *J. Phys. Chem. B* **2001**, *105*, 4827–4839.

MA020784W